Journal of the Korean Nuclear Society
Volume 26, Number 1, March 1994

Thermal-Hydraulic Analysis and Parametric Study on the Spent Fuel Pool Storage

Kye Bock Lee, Ki Il Nam, Jong Ryul Park, and Sang Keun, Lee
Korea Atomic Energy Research Institute
(Received August 2, 1993)

기사용 핵연료 저장조에 대한 열수력 해석 및 관련 인자의 영향 평가

이계복 · 남기일 · 박종률 · 이상근
한국 원자력 연구소
(1993. 8. 2 접수)

Abstract

The objective of this study is to conduct a thermal-hydraulic analysis on the spent fuel pool and to evaluate a parametric effect for the thermal-hydraulic analysis of spent fuel pool. The selected parameters are the Reynolds Number and the gap flow through the water gap between fuel cell and fuel bundle.

The simplified flow network for a path of fuel cells is used to analyze the natural circulation phenomenon. In the flow network analysis, the pressure drop for each assembly from the entrance of the fuel rack to the exit of the fuel assembly is balanced by the driving head due to the density difference between the pool fluid and the average fluid in each spent fuel assembly. The governing equations were developed using this relation. But, since the parameters(flow rate, pressure loss coefficient, decay heat, density)are coupled each other, iteration method is used to obtain the solution. For the analysis of the YGN 3&4 spent fuel rack, 12 channels are considered and the inputs such as decay heat and pressure loss coefficient are determined conservatively.

The results show the thermal-hydraulic characteristics(void fraction, density, boiling height)of the YGN 3&4 spent fuel rack. There occurs small amount of boiling in the cells. Fuel cladding temperature is lower than 343. 3°C. The evaluation of parametric effect indicates that flow resistances by geometric effect are very sensitive to Reynolds number in the transition region and the gap flow is negligible because of the larger flow resistance in the gap flow path than in the fuel bundle.

요 약

기사용 핵연료 저장조에 대한 열수력 해석과 관련된 인자들이 열수력 해석에 미치는 영향에 대한 분석

을 수행하였다. 기사용 핵연료에서 발생하는 붕괴열(decay heat)을 제거하기 위해 일어나는 자연 순환(natural circulation)현상을 모사하기 위해 단순화된 유동망(simplified flow network)해석 모델을 사용하였다. 기사용 핵연료 저장조의 각 셀에 저장되는 연료 집합체에서 발생하는 붕괴열을 제거하기 위해 흐르는 유량의 압력 손실량이 자연순환을 일으키는 밀도차이에 의해 생성되는 구동력(driving force)과 평형을 이루는 관계를 이용하여 지배 방정식을 유도하였다. 그러나 유량, 저항 계수, 붕괴열, 밀도 등의 변수들이 서로 종속 관계를 갖기 때문에 반복 계산을 통해 해를 얻게 된다. 본 해석을 적용한 영광 3, 4호기의 경우, 12 채널을 고려하였고 사용되는 입력 (저항 계수, 붕괴열)을 보수적으로 결정하였다.

본 연구를 통해 영광 3, 4호기 기사용 핵연료 저장조의 열수력 특성을 구하였다. 또한 유동로를 따라 형성되는 유동 저항중에 기하학적 요인에 의한 압력 손실은, 기사용 핵연료 저장조의 경우 압력 용기내의 유동과 달리 천이 영역(transition region)이 존재하게 되므로 Reynolds수에 민감한 것을 알 수 있다. 간극 유동은 조밀화된 연료 집합체 (consolidated fuel assembly)가 아닌 경우 무시할 수 있었다.

1. Introduction

The storage of spent fuel from nuclear power reactors has recently been a major concerns. In 1977, Battelle-Pacific Northwest Laboratories issued a report included a survey of U.S.A. and Canadian spent fuel storage experiences[1,2]. There has been no evidence that the fuel has been degraded during pool storage, based principally on visual observations and radiation monitoring of pool air and water. Perceptions regarding the status of the stored spent fuel are based on visual observations during fuel handling operations and on visible portions of the bundles during storage.

The principal goal in the design of underwater storage systems is assuring removal of heat generated in the spent fuel by radioactivity decay. The methods used to provide cooling for the removal of decay heat from the stored assemblies vary from plant to plant depending upon the design. The safety function to be performed by the system in all cases are the same: that is, the spent fuel assemblies must be cooled and must remain covered with water during all storage conditions.

The adequacy of natural convection is assured through thermal-hydraulic analyses involving the heat output from the spent fuel, the hydraulic resistance in various parallel flow paths of the fuel bundles, and flow resistance encountered by water circulating through the supporting structure and the orifices incorporated in the structure to achieve suitably balanced flow in a partially-filled storage array[3].

If spent fuel storage facilities are not located within the primary reactor containment or provided with adequate protective features, radioactive materials could be released to the environments as a result of either loss of water from the storage pool or mechanical damage to fuel within the pool. Regulatory guidance for the storage rack at nuclear reactors is based on Regulatory Guide 1.13[4] and 10 CFR 50[5].

From the SRP(NUREG-0800)[6], the spent fuel assemblies must be cooled and must remain covered with water during all storage conditions. Practically, the thermal-hydraulic criteria for the spent fuel rack design are defined as follows[7]:

The spent fuel pool stroage racks are designed to prevent extensive bulk boiling in the racks as well as maintain fuel caldding temperature well below 343.3°C.

Figures 1 and 2 represent the YGN 3&4 spent fuel stroage rack assembly which consists of nine individual spent fuel stroage rack modules arranged in the spent fuel storage pool[8]. The spent fuel is covered with 7.32 meters of water above the fuel racks in the normal condition.

The spent fuel storage racks are designed for the

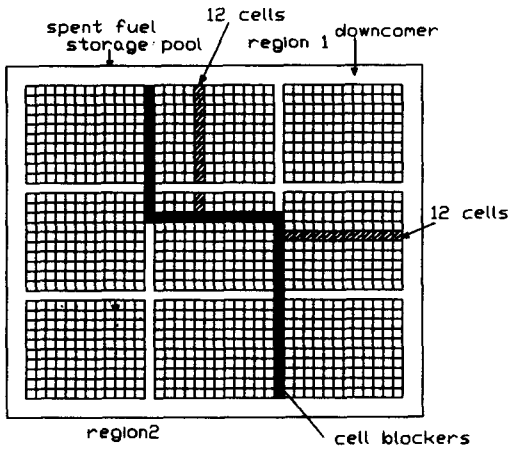

Fig. 1. Spent Fuel Pool Layout(top view)
region 1 : 50% storage
region 2 : 75% storage

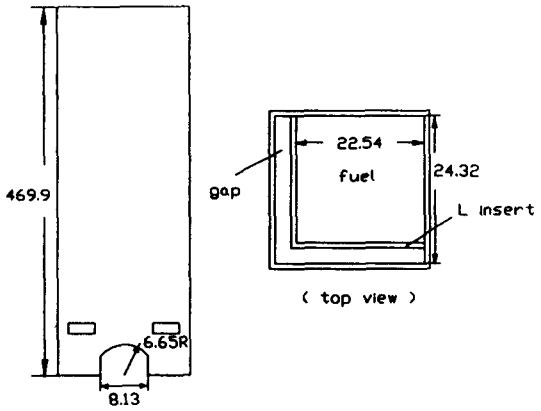

Fig. 2. Typical Cell in the YGN 3&4 Spent Fuel Rack (dimensions in cm)

minimum storage of 10 years of discharged fuel assemblies plus one full core of fuel assemblies. Nine 10×12 modules having a usable total capacity 678 fuel assemblies are provided. The spent fuel storage area is divided into two regions; Region 1 is composed of 246 cavities in a 50% dense storage configuration, the freshly discharged spent fuels are stored in this region; Region 2 is composed of 432 cavities in a 75% dense storage configuration, the depleted spent fuels are stored in this region. Coolant from the spent fuel pool enters horizontally at the bottom region of the spent fuel stroage rack and proceeds towards the remotest assembly. At each fuel cell, part of the horizontal flow turns and flows vertically through the spent fuel assembly stored there.

Driving head for the flow is supplied by the difference between the pool fluid density and the average fluid density in each spent fuel assembly. The convective flow rate is determined by balancing the driving force and pressure loss due to the flow resistance along the flow path.

The convective flow rate is determined by balancing the driving force and pressure loss due to the flow resistance using the iteration method. First, the convective flow rate is assumed. The enthalpy at the exit of the fuel assemblies is calculated based on the spent fuel decay heat. Driving force is calculated based on the difference between the pool fluid density and average fluid density in each spent fuel assembly. Using the assumed convection flow rate, pressure loss along the flow path can be calculated and compared with driving force. The convective flow rate is adjusted by comparison of driving force and pressure loss. Fuel cladding temperature is calculated by water temperature and flow rate determined above.

The important parameters for the thermal-hydraulic analysis are the heat generation rate in the hottest spent fuel assembly, inlet temperature at the bottom of the rack and the flow resistance in the system. Particularly, the flow resistances by the geometric effect are very sensitive to Reynolds number in the transition region (laminar→turbulent). Therefore, in this paper, this effect on the spent fuel rack thermal-hydraulic analysis is studied.

The objective of this study is firstly to perform the thermal-hydraulic analysis of the YGN 3&4 spent fuel assemblies in the pool and to evaluate a parametric effect of the flow resistances.

2. Flow Network Analysis

To perform the thermal-hydraulic analysis, the flow network has been developed for a path of fuel cells, leading to the remotest assembly in the racks.(Fig.3) Each vertical line represents a fuel cell. The last cell represents the remotest assembly in the rack (located at the center of the rack).

From the Fig.1, 12th cell, being farthest from the pool wall, is the hottest in the region 1. Coolant reaching this cell experiences the greatest resistance in the flow circulation loop, therefore, the coolant in this cell must be the hottest to create the largest density difference to overcome this resistance and drive flow to this assembly. Thus, 12 cells are considered in this analysis.

In the flow network analysis, for each assembly, the pressure drop from the entrance of the fuel rack to the exit from the fuel assembly is balanced by the driving head which is a function of the spent fuel assembly flow rate and the assembly heat generation rate. The equations for the flow network are as follows:

$$\Delta P_1 = \Delta P_p + L_c[\rho_o - \rho_1(Q_1,W_1)] = [W_o^2 R_A + W_1^2 R_{B1}(Q_1,W_1)]/2g_c + \Delta P_d \quad (1)$$

$$\Delta P_2 = \Delta P_p + L_c[\rho_o - \rho_2(Q_2,W_2)] = [W_o^2 R_A + (W_0 - W_1)^2 R_c + W_2^2 R_{B2}(Q_2,W_2)]/2g_c + \Delta P_d \quad (2)$$

$$\Delta P_i = \Delta P_p + L_c[\rho_o - \rho_i(Q_i,W_i)] = [W_o^2 R_A + \sum_{k=1}^{i-1}[(W_0 - \sum_{j=1}^{k} W_j)^2]R_c + W_i^2 R_{Bi}(Q_i,W_i)]/2g_c + \Delta P_d \quad (3)$$

$$\Delta P_L = \Delta P_p + L_c[\rho_o - \rho_L(Q_L,W_L)] = [W_o^2 R_A + \sum_{k=1}^{L-1}[(W_0 - \sum_{j=1}^{k} W_j)^2]R_c + W_L^2 R_{BL}(Q_L,W_L)]/2g_c + \Delta P_d \quad (4)$$

$$W_L = W_o - \sum_{j}^{L-1} W_j \quad (5)$$

where,

- ΔP_i : pressure loss across each cell
- L_c : length of the cell
- ρ_o : average density of the pool water in the downcomer
- ρ_i : average density of the coolant in each cell
- W_o : flow rate through the downcomer entering the first cell
- W_i : flow rate in each cell
- W_L : flow rate in the last cell
- Q_i : heat generation rate in each cell
- R_A : total resistance at the entrance of the first cell
- R_{Bi} : total cell resistance
- R_c : bottom cell resistance in the flow path under the cells
- g_c : gravitational constant
- ΔP_d : pressure drop through downcomer
- ΔP_p : pressure rise due to circulating pump

The parameters ρ_i and R_{Bi} are determined by heat generation rate and flow rate of each cell. Changes in Q_i, W_i will vary the density and cell resistances for each cell.

For single phase flow, the average density in the active portion of the fuel assembly is the arithmetic average of the densities corresponding to the bottom and top of the active fuel. For two phase flow, the average density is the arithmetic average of the average density in the non-boiling height and the boiling height.

The evaluation of the average density is based upon the heat generation rate in the assembly, the cell flow rate, the inlet temperature and the pressure in the pool. The pressure in the pool is basically controlled by the height of the water in the pool and the average density of the pool. The pressure rise due to the pumps in this study is neglected. This assump-

tion will add conservatism to the results because the flow rates will be smaller in the cells.

There are (L+1) equations and (L+1) unknowns (W_0, W_1 ···, W_L). These (L+1) equations are solved simultaneously. Given the heat generation rate and dimensions of the system, the water flow rate induced by natural circulation can be calculated using theoretical or empirical flow resistance coefficients.

3. Evaluation of Flow Network Equations

3.1. Average density in each cell

Assume that the inlet temperature(T_0)is 65.6°C and the flow rate(W)is 0.572kg/sec, then the enthalpy at the inlet of cell is determined from the steam table[9] at 206.8kN/m², the assumed pressure at the inlet of cell.

$$h_0 = 274.5 \text{ (kJ/kg)}$$

The enthalpy at the exit of active fuel bundle, he, is determined using the heat generation rate;

$$he = h_0 + Q/W = 490.3 \text{ (kJ/kg)}$$

Q is the maximum spent fuel bundle heat generation rate at the minimum of 3 days after shutdown(appendix B).

For the case of boiling in the cell the following relations are used;the average density in the non-boiling height ρ_{NB},

$$\rho_{NB} = (\rho_0 + \rho_{Bi})/2 \quad (6)$$

where,

ρ_0 : density at the inlet of the cell

ρ_{Bi} : density at the beginning of the boiling height at saturated condition

the average density in the boiling height, ρ_B

$$\rho_B = (\rho_{Bi} + \rho_{Be})/2 \quad (7)$$

where,

ρ_{Be} : density at the exit of the boiling height end of active fuel

$$\rho_{Be} = (1-\alpha_e)\rho_{fe} + \alpha_e \rho_{ge} \quad (8)$$

ρ_{fe} : density of saturated liquid at the exit of the active fuel

ρ_{ge} : density of saturated vapor at the exit of the active fuel

α_e : void fraction at the exit of active fuel with an assumed slip ratio of 4[10]

$$\alpha_e = \frac{\chi_e (1/s) (\rho_{fe} / \rho_{ge})}{[(1-\chi_e) + \{ \chi_e (1/s) (\rho_{fe} / \rho_{ge}) \}]} \quad (9)$$

χ_e : exit quality($=(h_{Be} - h_{fe})/h_{fg}$)

h_{Be} : enthalpy at boiling exit

h_{fe} : saturated liquid enthalpy at boiling exit

h_{fg} : $h_{ge} - h_{fe}$

s : slip ratio

Assume the pressure at the exit of active fuel bundle, $P_e = 172.4 (kN/m^2)$, then, from above relations, $\chi_e = 0.0024$, $\alpha_e = 0.367$

$$\rho_{Be} = 599.38 \text{ (kg/m}^3\text{)}$$

To estimate the non-boiling and boiling height in the fuel bundle, assume enthalpy increases linearly up to the channel. Since enthalpy and density of saturated water at 172.4(kN/m²) are 485.0(kJ/kg) and 946.3 (kg/m³), we can obtain $L_{NB} = 3.72$ (m) $L_B = 3.65$(m)

Thus, from equations (6) and (7),

The density above the fuel bundle in the rack is assumed to be same as ρ_{Be} since no heat is added in this region.

Therefore, the average density in the cell is

$$\rho_C = \frac{\rho_{NB} L_{NB} + \rho_B L_B + \rho_{Be} L_T}{L_{NB} + L_B + L_T} \quad (10)$$

where, L_T is the length above the active fuel in the rack.

From the equation (10), $\rho_c = 907.32(kg/m^3)$

To calculate the average density of water above the racks, the average cell flow rate from all the cells in the rack is needed. Since it is difficult to determine the average flow rate for all cells, an average cell flow rate is assumed based on the previous spent fuel rack calculations.

Assume $W_{avg} = 0.544(kg/sec)$, $P = 165.5(kN/m^2)$ and using average bundle heat generation rate 10.38 kW,

$$h = h_o + Q/w = 293.4(kJ/kg)$$

then, the average density above the rack in the pool, $\rho_{TT} = 977.89(kg/m^3)$

Thus, the average density in the pool is,

$$\rho_p = \frac{\rho_{NB}L_{NB} + \rho_B L_B + \rho_{BO}L_T + \rho_{TT}L_{TT}}{L_{NB} + L_B + L_T + L_{TT}} \quad (11)$$

where L_{TT} is the length above the rack in the spent fuel pool. Using equation (11), $\rho_p = 951.22(kg/m^3)$

The pressure in the pool is basically controlled by the height of the water in the pool and the average density in the pool. Thus, the pressure increases as a function of depth according to the following formula,

$$P(Y) = 101.35 + g \times \rho_p \times Y/1000 \quad (12)$$

where,

Y : the depth of water above the point where the pressure is being calculated, meter

ρ_p : average pool density, kg/m^3

P(Y) : pressure at depth Y, kN/m^2

g : gravitational constant

The above procedure is repeated until the average density in the pool is the same as that recalculated after iteration. In this case, the final average density in the pool is $949.94(kg/m^3)$.

Using the above pressure equation and steam tables, saturated enthalpy curves are plotted as a function of distance from the bottom of the active core in Fig.4. From this figure the boiling height and non-boiling height are estimated by knowing the enthalpy at the inlet of the cell and the enthalpy at any point in the spent fuel. A line is drawn from the inlet and any point enthalpy in the active core to determine the intersection with the saturated enthalpy curve in Fig.4. This intersection represents the beginning of the boiling section in the active region of the cell.

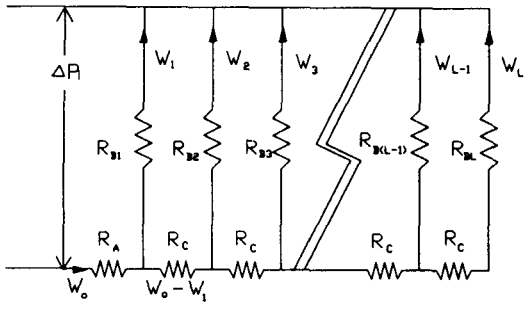

Fig. 3. Flow Network

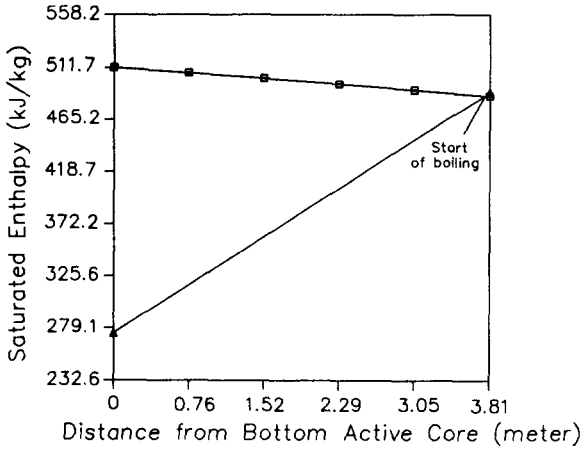

Fig. 4. Saturated Enthalpy vs. Distance

3.2. Flow resistance in each cell

Along the flow path, pressure drop occurs by friction loss, form loss (geometric effect). Fig.5 represents a schematic diagram of the flow path in the spent fuel cell showing the location of what is termed cell station. In proceeding station 1 to station 8, one follows the coolant flow path through the spent fuel cell. Regions used in the pressure loss calculations are identified by the use of the station numbers representing the limits of the region.

Hydraulic calculations use the dimensionless coefficient of fluid resistance, which conveniently has the same value in dynamically similar flows, that is, flows over geometrically similar regions and with equal Reynolds numbers or other pertinent similarity criteria, irrespective of the kind of fluid or the flow velocity and dimensions of the segments being calculated.

Expressions used for frictional and geometric pressure losses are taken from the literature[11,12]. They are based on the use of standard pressure loss correlations for frictional and geometric losses (contraction, expansion and orifice losses). Flow resistances are determined for laminar, turbulent and boiling condition.

The pressure loss by the geometric effect in a flow region is in all cases a function of the configuration, directly or indirectly; indirectly in that it is flow dependent and this flow depends on geometry; directly in that pressure loss coefficients vary with configuration and direction of flow. These are caused by the following: local disturbances of the flow, separation of flow from the walls and the formation of vortices and strong turbulent agitation of the flow at places where the configuration of the pipeline changes or fluid streams meet or flow past obstruction(entrance of a fluid into the pipeline, expansion, contraction, bending and branching of the flow, flow through orifices, grids or valves, etc.).

In practice, the effect of the Reynolds number on the geometric loss is mainly evident at its small values($Re \leq 10^4$)[11,12]. When $Re > 10^4$, the geometric loss coefficients may nearly always be assumed independent of the value of Reynolds number. At smaller value of Reynolds number, its effect should be taken into account.

When the flow area is constant and no bends are involved, the pressure drop is a function of shear at the bounding surfaces. This type of pressure loss is called frictional loss. The friction factor has been made into a group of correlations describing the variation of friction factor with Reynolds number for various values of relative roughness, as presented by Moody[13].

To study the effect of the Reynolds number which affects the form loss coefficient, two cases are considered in this paper. The one is assumed that the form loss coefficient is only dependent on the configuration. In this case, the correlations for turbulent flow are used. The other case is assumed that the form loss coefficient depends on the configuration and the flow characteristics. The detailed form loss

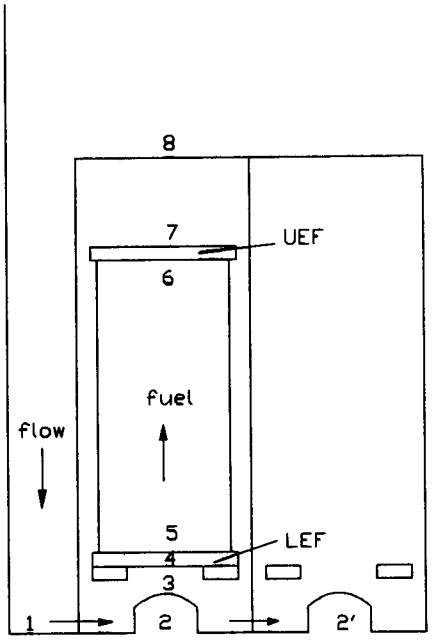

Fig. 5. Flow Path Stations

Table 1. The Flow Resistance Type along the Flow Path in Each Case

Stations	Pressure Loss Type	Case 1	Case 2
1−2	Contraction & Expansion (Form Loss)	F(geometry) K = 1.102	F(geometry, Re) k = 2.128 Re = 1.0(10^4)
2−2′	Contraction & Expansion (Form Loss)	F(geometry) k = 0.990	F(geometry, Re) k = 1.719 Re = 1.0(10^4)
2−3	90° turn	k = 1.13	k = 1.13
3−4	Contraction & Expansion (FormLoss)	F(geometry) k = 0.662	F(geometry, Re) k = 0.890 Re = 1.0(10^2)
4−5	Contraction & Expansion(LEF) (Form Loss)	F(geometry) k = 0.388	F(geometry, Re) k = 0.405 Re = 1.0(10^2)
5−6	Friction Loss −friction −spacer grid	F(Re, ϵ) CE correlation Re = 1.0(10^3)	F(geometry, ϵ) CE correlation Re = 1.0(10^3)
6−7	Contraction & Expansion(UEF) (Form Loss)	F(geometry) k = 1.094	F(geometry, Re) k = 1.094 Re = 1.0(10^4)
7−8	Expansion (Form Loss)	F(geometry) k = 1.30	F(geometry) k = 1.30
Downcomer	Friction 90° turn	F(Re, ϵ) k = 1.13 Re = 1.0(10^5)	F(Re, ϵ) k = 1.13 Re = 1.0(10^5)

coefficient for each case is attached in the appendix A.

Table 1 lists the type of pressure loss for each case and each station number of the flow path is shown in Fig. 5.

4. Results and Discussion

4.1. Thermal-hydraulic analysis

Equations for the flow network are solved to give the flow rates in the cells. The average density, flow resistance and the void fraction for each cell are also calculated. The iteration is performed until the driving force is balanced by the pressure loss due to flow resistance.

The results for all cases are shown in tables 2 and 3. They represent flow rate, flow resistance, average density, boiling and non-boiling core height, cell exit void fraction in each cell.

Results in tables 2 and 3 indicate there is a small amount of boiling, when the assembly heat gener-

ation rate is 123.3 kW in each cell. Based on the following conservatism it is assumed that this small amount of boiling will be decreased or negligible in the pool.

- The maximum assembly heat generation rate could actually be lower for some of the cells in the flow network(using maximum peaking factor).
- Additional flow from the long side of the spent fuel racks is neglected.
- The pump pressure rise is neglected in the flow network equation.
- Conservatism is applied in evaluating some of the resistance in the flow network.
- Practically, the spent fuels are partially filled in the

Table 2. Thermal-hydraulic Results in Each Cell for Case 1

Cell No.	Flow rate (kg/sec)	Heat Rate (kW)	Non-boiling Height (m)	Boiling Height (m)	Pool Density (kg/m^3)	Cell Density (kg/m^3)	Exit Void Fraction
1	0.5762	123.3	3.809	.001	980.25	959.62	.0068
2	0.5737	123.3	3.790	.020	980.25	944.62	.1164
3	0.5713	123.3	3.772	.038	980.25	932.27	.2035
4	0.5690	123.3	3.755	.055	980.25	922.26	.2713
5	0.5670	123.3	3.741	.069	980.25	914.40	.3225
6	0.5652	123.3	3.728	.082	980.25	908.37	.3604
7	0.5638	123.3	3.718	.092	980.25	903.96	.3872
8	0.5628	123.3	3.711	.099	980.25	900.89	.4054
9	0.5621	123.3	3.707	.103	980.25	898.92	.4169
10	0.5618	123.3	3.704	.106	980.25	897.83	.4233
11	0.5616	123.3	3.703	.107	980.25	897.33	.4262
12	0.5615	123.3	3.703	.107	980.25	897.20	.4269

Table 3. Thermal-hydraulic Results in Each Cell for Case 2

Cell No.	Flow rate (kg/sec)	Heat Rate (kW)	Non-boiling Height (m)	Boiling Height (m)	Pool Density (kg/m^3)	Cell Density (kg/m^3)	Exit Void Fraction
1	0.5736	123.3	3.789	.021	980.25	943.74	.1227
2	0.5682	123.3	3.749	.061	980.25	918.76	.2944
3	0.5619	123.3	3.705	.105	980.25	898.26	.4208
4	0.5556	123.3	3.662	.148	980.25	881.81	.5098
5	0.5497	123.3	3.623	.187	980.25	868.87	.5710
6	0.5447	123.3	3.590	.220	980.25	859.03	.6122
7	0.5409	123.3	3.565	.245	980.25	851.84	.6395
8	0.5381	123.3	3.547	.263	980.25	846.85	.6571
9	0.5363	123.3	3.535	.275	980.25	843.68	.6678
10	0.5352	123.3	3.528	.282	980.25	841.88	.6736
11	0.5348	123.3	3.525	.285	980.25	841.10	.6761
12	0.5347	123.3	3.525	.285	980.25	840.90	.6767

storage rack (Fig.1).

From the tables 2&3, the parametric study on the spent fuel pool thermal-hydraulic analysis reveals that the flow resistances, such as loss coefficients to entrance of the inlet hole of the first cell and for the bottom inlet hole losses under the cells, are sensitive to Reynolds number in the transition region. Thus, the pressure loss coefficient correlations for the flow resistance by the geometric effect have to be chosen carefully according to the flow conditions(laminar or turbulent).

4.2. Determination of maximum cladding surface temperature

Maximum cladding surface temperature is determined with the maximum heat flux and the maximum possible coolant temperature that could exist in the spent fuel rack. The heat transfer coefficient at the spent fuel is calculated using the laminar forced convection correlation[10];

$$h_c = \frac{k}{D_e} 1.86 \left[\frac{Re\ Pr\ D_e}{L} \right]^{0.33} \left(\frac{\mu_b}{\mu_s} \right)^{0.14} \quad (13)$$

where, L : length of heated path

P_r : Prandtl Number($C_p\mu/k$)

μ_b : bulk coolant viscosity

μ_s : surface viscosity

k : thermal conductivity

C_p : specific heat

Maximum coolant temperature can occur at the inlet of active fuel at saturation conditions with the maximum pool height. Pressure at the inlet of pool with maximum pool height from case 1 is P=210.83(kN/m^2). Therefore, at that pressure, saturation temperature, T_{sat}, is 121.11°C. This temperature is very conservative.

The lowest flow rate before boiling beginning in the cell is 0.5443 (kg/sec), thus,

$$Re = \frac{D_e \times W}{A \times \mu_b} = 1137 \quad \text{(laminar flow)}$$

Assume $\mu_s = \mu_b$,

substitution of Re, and all preperty values into equation (13) results in

$$h_c = 158.47\ (W/m^2 \cdot {}^\circ F)$$

From the following relation,

$$Q'' = h_c\ (T_{clad} - T_b) \quad (14)$$

where Q" is the maximum local heat flux(appendix B), T_b is bulk temperature.

we can obtain,

$T_{clad} = 162.87°C$

Therefore, maximum cladding surface temperature is lower than 343.3°C(650°F).

4.3. Gap flow effect

The gap flow through the water gap between fuel cell and fuel bundle is considered to check the effect on the thermal-hydraulic analysis in the spent fuel rack. In a fuel cell, the gap flow, bypassing the fuel region, is assumed to be at the same temperature as in the fuel region.

The flow network is developed for the gap and fuel bundle in Figure 6.

R_g : flow resistance through gap ($=k_g/(A_g^2\rho)$)

R_B : flow resistance through fuel bundle

R_c : flow resistance under the cell

R_n : residual flow resistance in the cell

W_T, W_g, W_B : total, gap, and bundle flow

Since pressure drops through the fuel bundle and gap are equal,

$$R_g W_g^2 = R_B W_B^2 \quad (15)$$

$$W_g + W_B = W_T \quad (16)$$

therefore,

$$W_B = \frac{W_T R_g^{1/2} (R_g^{1/2} - R_B^{1/2})}{(R_g - R_B)} \quad (17)$$

therefore,

The flow resistance for the gap and fuel bundle flow path is calculated to compare the flow rate in each flow path for the YGN 3&4. Since the gap exit flow area is flapped, the gap flow resistance is larger than the fuel bundle resistance. The estimated loss coefficient in the gap flow path is $k_{gap}=49$ and that in the fuel bundle flow path is $k_{bundle}=32$[11]. From the equation (15), the ratio of the flow rate, W_g/W_T is 0.1. The gap flow through the water gap between the fuel cell and fuel bundle is small compared to the fuel bundle flow. Therefore the gap flow is negligible. The negligence of the gap flow imposed a conservatism to the thermal-hydraulic results.

However, the consolidated fuel cell of lower decay energy than the intact fuel has a much larger flow resistance where the flow is more restricted in the densely packed fuel region than the gap region.

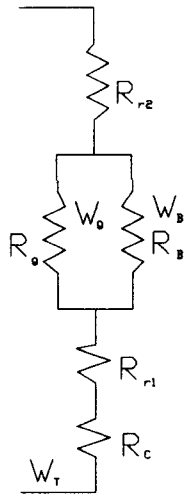

Fig. 6. Gap flow Network

Thus, the adverse cooling effect due to gap flow in a consolidated cell has to be considered.

5. Conclusion

In order to assess the cooling adequacy on the YGN 3&4 spent fuel rack, a simplified flow network model, which simulates the natural circulation phenomenon in the spent fuel pool, has been presented, and the sensitivity study on the parameters which have an effect on this analysis were performed.

Results indicate that there is a small amount of boiling. But, this small amount of boiling is neglgible because of the conservatism included in the analysis. Maximum cladding surface temperature is lower than 343.3°C(650°F).

From the parametric study, it was known that flow resistances by geometric effect are sensitive to Reynolds number in the laminar and transition region, and the gap flow in the intact fuel is negligible.

References

1. A.B. Johnson, Jr., "Spent Fuel Storage Experience," Nuclear Technology, Vol. 43, p.165, (1979)
2. A.B. Johnson, Jr., Behavior of Spent Nuclear Fuel in Water Pool Storage, BNWL-2256, (1977)
3. M.E. Weech and Y.J. Lee, "Heat Transfer in Spent Fuel Storage," Nuclear Engineering and Design, Vol. 67, p.379, (1981)
4. USNRC Regulatory Guide 1.13, Spent Fuel Stroage Facility Design Basis, (1981)
5. USNRC NUREG-0800, Spent Fuel Pool Cooling and Cleanup System, Rev. 01, July, (1981)
6. Code of Federal Regulations, 10 CFR 50 Appendix A, (1991)
7. YGN 3&4 Preliminary Safety Analysis Report. Vol. 6, (1988)

8. ABB－CE Drawings,
－Spent Fuel Pool Proposed Arrangement (SE－10487－630－105)
－Spent Fuel Rack Module Assembly (E－10287－666－002)
9. C.A. Meyer, R.B. McClintock, G.J. Silvestri and C. Spencer Jr., ASME Steam Tables, The American Society of Mechanical Engineers, (1983)
10. F. Kreith, Principles of Heat Transfer, Intext Education Publishers, (1973)
11. I.E. Idelchik, Handbook of Hydraulic Resistance, Hemisphere Publishing Corporation, (1986)
12. F.J. Staron and R.H. Vickerman, REVEL, A Computer Code to Calculate Nozzle to Nozzle Pressure Drop, C－E Combustion Division
13. L.F. Moody, "Friction Factors for Pipe Flow," ASME, Vol. 66, (1944)

Appendix A

Flow resistance and geometry data

1. Bundle resistance (case 1&2)

friction

$f = 64/Re$, for laminar flow

f: from Moody diagram, for turbulent flow

spacer grids[12]

$k_{inconel} = 1.52(Re)^{-0.0777}$

$k_{HID} = N(3.049)\ (Re)^{-0.1401}$

N is the number of the Zircaloy spacer grids

Resistances in the boiling height where two phase flow exists are calculated by assuming that the fluid is a saturated liquid and then a correction factor is applied to account for the two phase effect.

2. Expansion resistance(case 1)

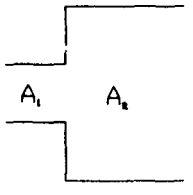

$$k_{1\text{-}2)1} = [\ 1 - (A_1/A_2)\ ]^2$$

3. Contraction resistance(case 1)

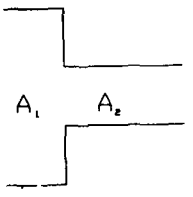

$$k_{1\text{-}2)2} = 0.5[\ 1 - (A_2/A_1)\ ]$$

4. Loss coefficient for orifice with sharp edges for different condition in the transient and laminar condition(case 2)

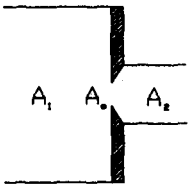

$$30 < Re < 10^4 \sim 10^5$$

$$k_{1\text{-}2)1} = (\zeta_\varphi + \varepsilon_{oRe}\zeta_1)(A_1/Ao)^2$$

$$\zeta_\varphi = F(\ Re,\ Ao/A_1\ )$$

$$\zeta_1 = [\ 1+0.707(1-Ao/A_1)^{1/2}-(Ao/A_2)\ ]^2$$

$$\varepsilon_{oRe} = F'\ (\ Re\ )$$

Geometry data

bundle flow area $A_B = 0.0309(m^2)$

hydraulic diameter in bundle $D_B = 0.0146(m)$

active fuel length: 3.81(m)

length from end of active core to cell exit: 0.635(m)

flow area of mouse hole : $0.0055(m^2)$

hydraulic diameter in the mouse hole: 0.077(m)

gap flow area: $0.0309(m^2)$

gap exit flow area: $0.0011(m^2)$

hydraulic diameter in the gap: 0.0259(m)

$$Q = \frac{f \times P_c \times R_p}{N_{assy}}$$

Appendix B

Maximum bundle heat generation rate

where

Q : maximum bundle heat generation rate

f : fraction of decay heat after 3 days

P_c : core power

R_p : rod radial power factor

N_{assy} : the number of assemblies in the core

$$Q = \frac{0.005 \times 2815 \times 10^3 \times 1.55}{177} = 123.3\ (kW)$$

The evaluation of the rate of heat evolution from the spent fuel is accomplished by means of computer codes(ORIGEN 2) that calculate the cumulative fissions, transmutations and isotopic decay taking place during fuel irradiation and the radioisotope decay or spontaneous fission subsequent to shutdown of the reactor.

$$Q'' = \frac{f \times P_c \times R_p \times R_a}{N_{assy} \times A_{assy}} = 6618 \ (W/m^2)$$

Maximum local heat flux

where R_a : axial peaking factor 1.47

A_{assy} : total heat transfer area per assembly